Supporting Information

Several energetic MOFs based on the N-rich energetic materials and alkali metals: Towards high detonation performances and good stabilities

Guofeng Zhang,[a] Xue Hao,[a] Yongbin Zou,[a] Shichang Liu,[a] Junjie Wei,[a] Zhen Dong*[a] and Zhiwen Ye*[a]

[a] School of Chemistry and Chemical Engineering, Nanjing University of Science and Technology, Xiaolingwei 200, Nanjing 210094, PR China

*Corresponding Author: yezw@njust.edu.cn & dongzhen90@126.com

Table of Contents

1. X-ray crystallographic datas

$[Na^+(ATDT^-)(H_2O)_2]$:

Table S1. Crystallographic data for **$[Na^+(ATDT^-)(H_2O)_2]$**.

Empirical formula	$C_4H_7N_{12}NaO_2$
Formula weight	278.21
Temperature/K	223.00
Crystal system	orthorhombic
Space group	Pbca
a/Å	12.5111(4)
b/Å	6.5119(2)
c/Å	26.0556(7)
α/°	90
β/°	90
γ/°	90
Volume/Å^3	2122.78(11)
Z	8
ρ_{calc}g/cm^3	1.741
μ/mm^{-1}	1.578
F(000)	1136.0
Crystal size/mm^3	0.15 × 0.13 × 0.11
Radiation	CuKα (λ = 1.54178)
2Θ range for data collection/°	6.784 to 136.482
Index ranges	-15 ≤ h ≤ 14, -7 ≤ k ≤ 6, -31 ≤ l ≤ 31
Reflections collected	15454
Independent reflections	1927 [R_{int} = 0.0468, R_{sigma} = 0.0238]
Data/restraints/parameters	1927/0/188
Goodness-of-fit on F^2	1.070
Final R indexes [I>=2σ (I)]	R_1 = 0.0338, wR_2 = 0.0879
Final R indexes [all data]	R_1 = 0.0413, wR_2 = 0.0926
Largest diff. peak/hole / e Å^{-3}	0.20/-0.28

CCDC: 2378833.

$[K^+(ATDT^-)(H_2O)]$:

Table S2. Crystallographic data for **$[K^+(ATDT^-)(H_2O)]$**.

Empirical formula	$C_4H_5KN_{12}O$
Formula weight	276.30
Temperature/K	223.00
Crystal system	triclinic
Space group	P-1
a/Å	6.7583(2)
b/Å	7.8975(2)
c/Å	9.8534(3)

α/°	85.648(2)
β/°	73.651(2)
γ/°	87.923(2)
Volume/Å^3	503.13(3)
Z	2
ρ_{calc}g/cm^3	1.824
μ/mm^{-1}	4.827
F(000)	280.0
Crystal size/mm^3	0.13 × 0.12 × 0.11
Radiation	CuKα (λ = 1.54178)
2Θ range for data collection/°	9.376 to 158.122
Index ranges	-8 ≤ h ≤ 7, -9 ≤ k ≤ 10, -11 ≤ l ≤ 12
Reflections collected	6944
Independent reflections	2084 [R_{int} = 0.0483, R_{sigma} = 0.0429]
Data/restraints/parameters	2084/0/164
Goodness-of-fit on F^2	1.056
Final R indexes [I>=2σ (I)]	R_1 = 0.0391, wR_2 = 0.1035
Final R indexes [all data]	R_1 = 0.0480, wR_2 = 0.1105
Largest diff. peak/hole / e Å^{-3}	0.33/-0.44

CCDC: 2385568.

[Cs$^+$(ATDT$^-$)]:

Table S3. Crystallographic data for **[Cs$^+$(ATDT$^-$)]**.

Empirical formula	C4H3CsN12
Formula weight	352.09
Temperature/K	223.00
Crystal system	triclinic
Space group	P-1
a/Å	7.6704(2)
b/Å	8.0941(3)
c/Å	8.4392(3)
α/°	90.8660(10)
β/°	109.2380(10)
γ/°	92.4870(10)
Volume/Å3	493.98(3)
Z	2
ρcalcg/cm3	2.367
μ/mm‑1	3.750
F(000)	332.0
Crystal size/mm3	0.13 × 0.12 × 0.11
Radiation	MoKα (λ = 0.71073)
2Θ range for data collection/°	5.04 to 50.642

Index ranges	-9 ≤ h ≤ 9, -9 ≤ k ≤ 9, -10 ≤ l ≤ 10
Reflections collected	10547
Independent reflections	1790 [Rint = 0.0367, Rsigma = 0.0226]
Data/restraints/parameters	1790/0/154
Goodness-of-fit on F2	1.052
Final R indexes [I>=2σ (I)]	R1 = 0.0174, wR2 = 0.0434
Final R indexes [all data]	R1 = 0.0183, wR2 = 0.0438
Largest diff. peak/hole / e Å-3	0.87/-0.38

CCDC: 2376608.

2. IR and NMR Spectures

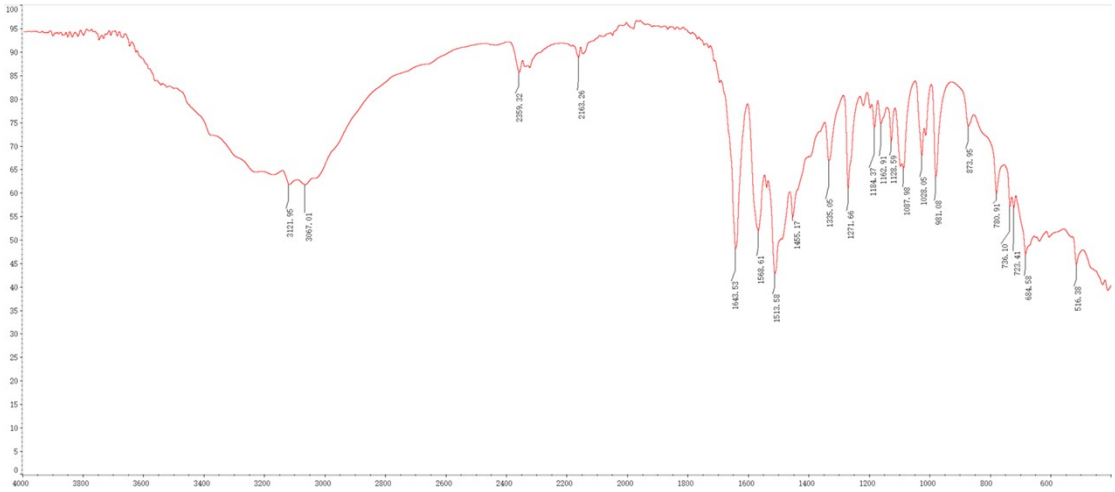

Figure S1. IR spectra of **ATDT–Li**.

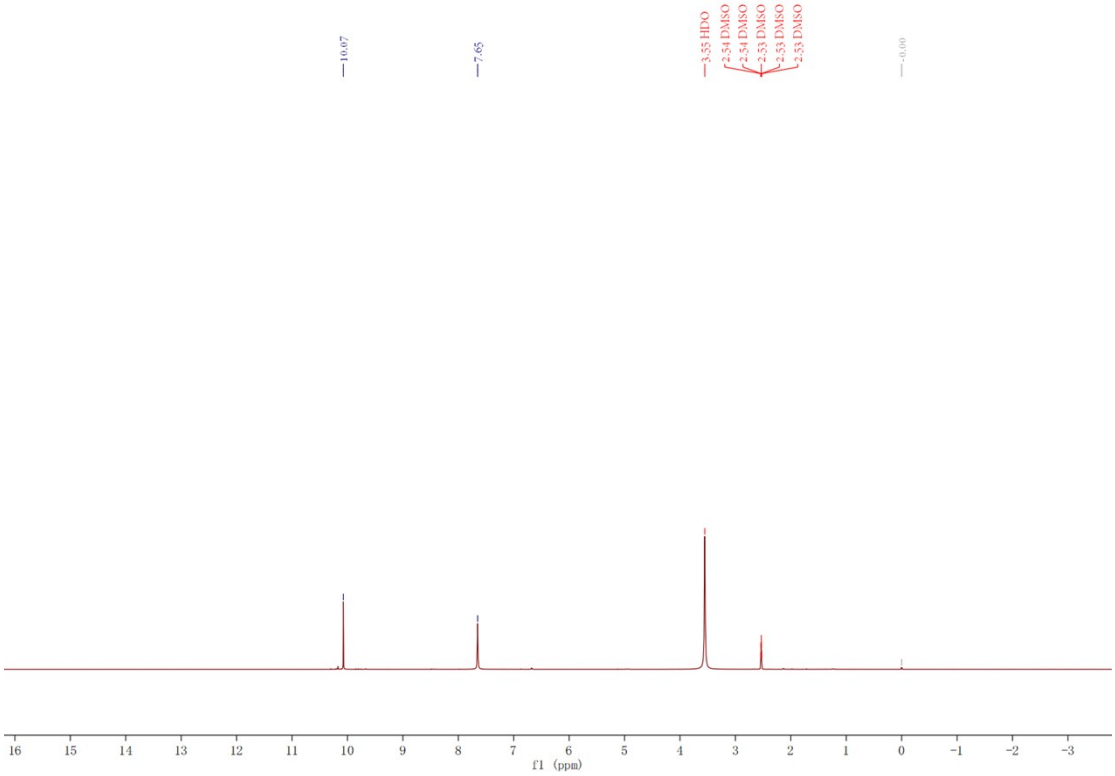

Figure S2. ^{1}H NMR spectra of **ATDT–Li**.

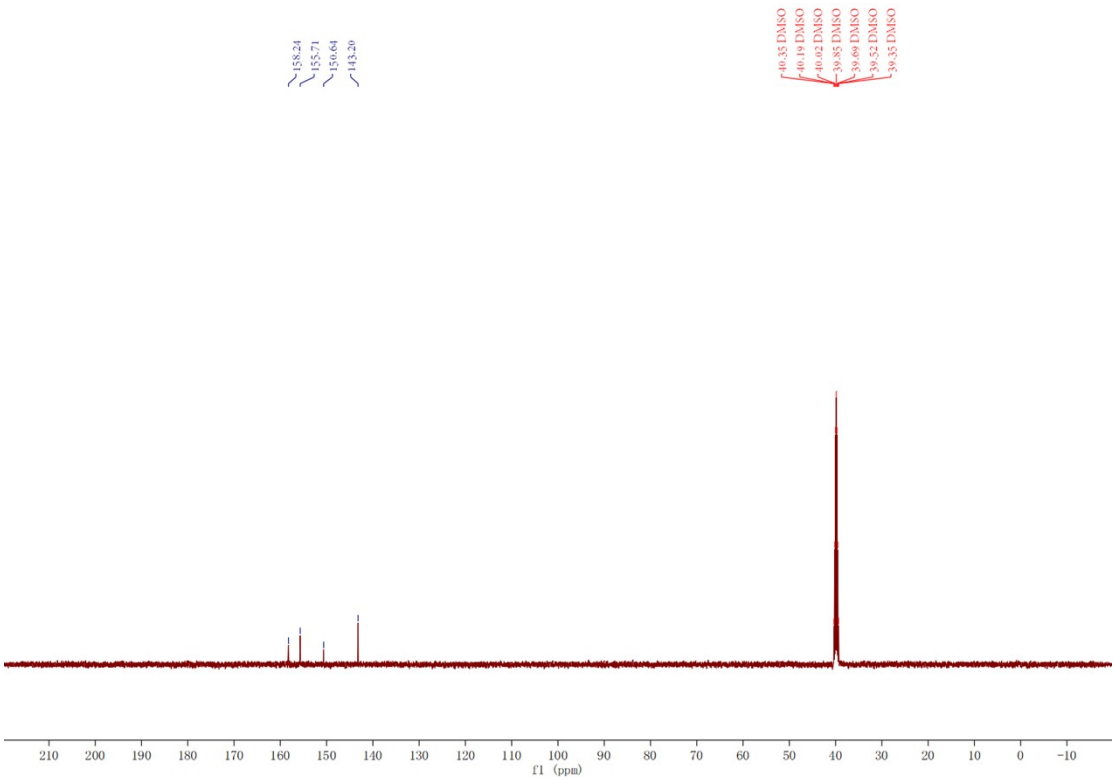

Figure S3. ^{13}C NMR spectra of **ATDT–Li**.

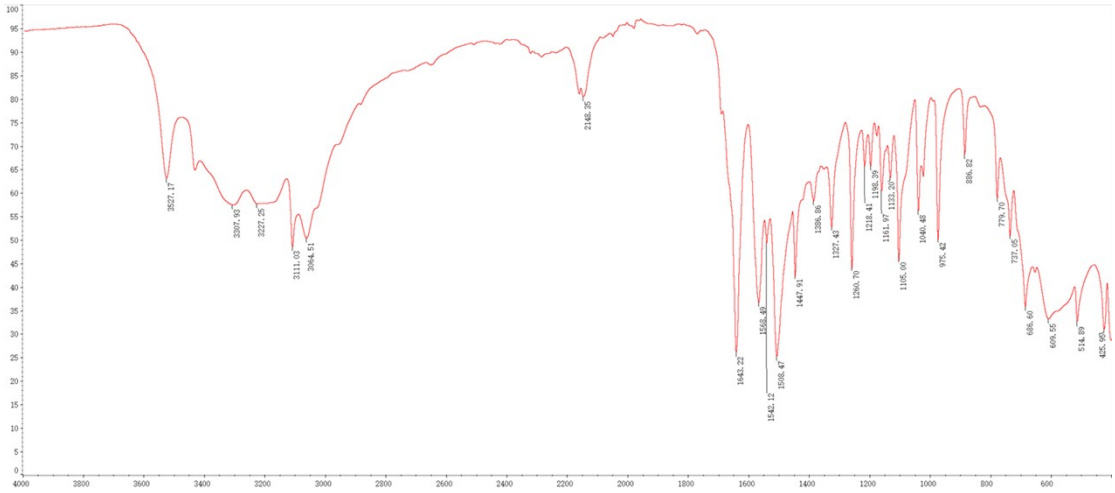

Figure S4. IR spectra of **ATDT–Na**.

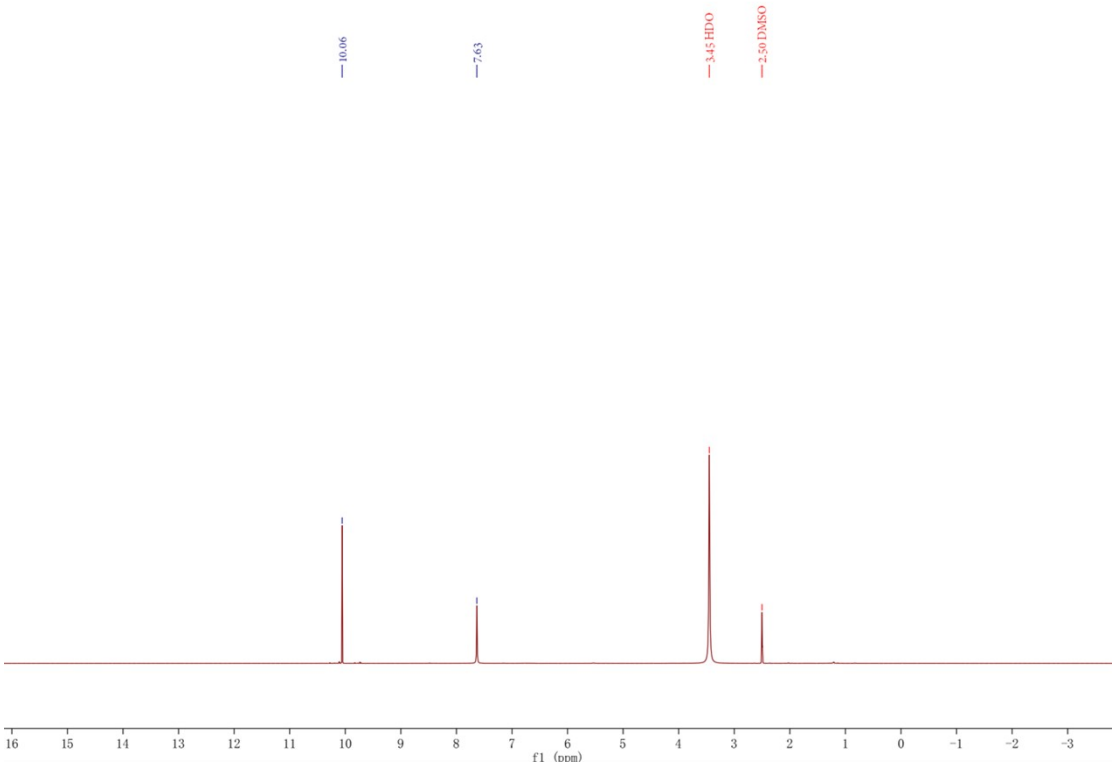

Figure S5. ^{1}H NMR spectra of **ATDT–Na**.

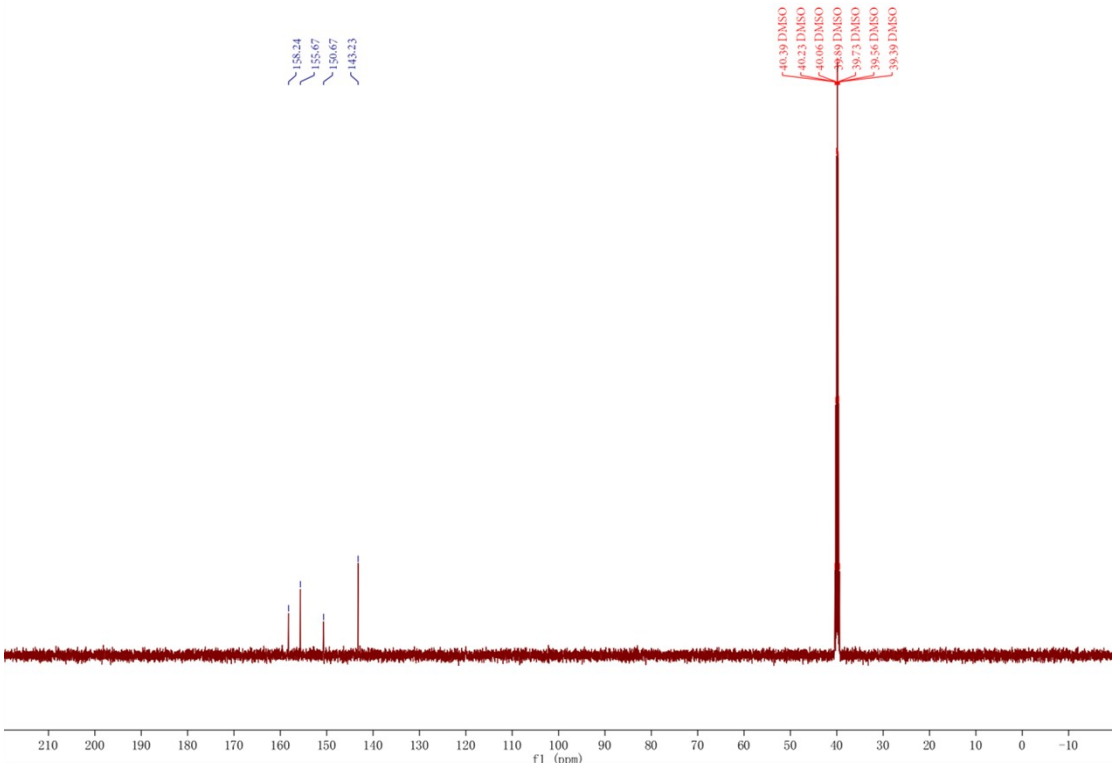

Figure S6. ^{13}C NMR spectra of **ATDT–Na**.

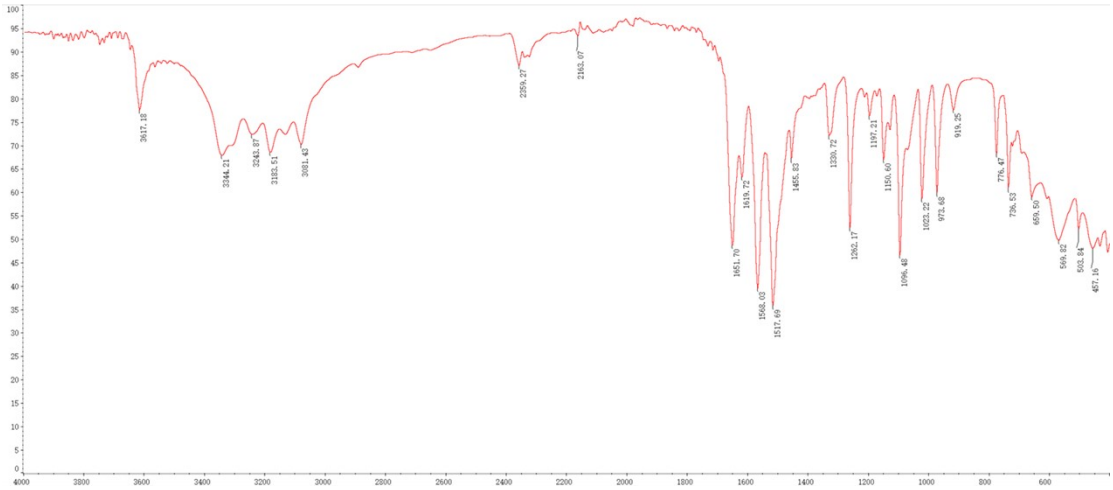

Figure S7. IR spectra of **ATDT–K**.

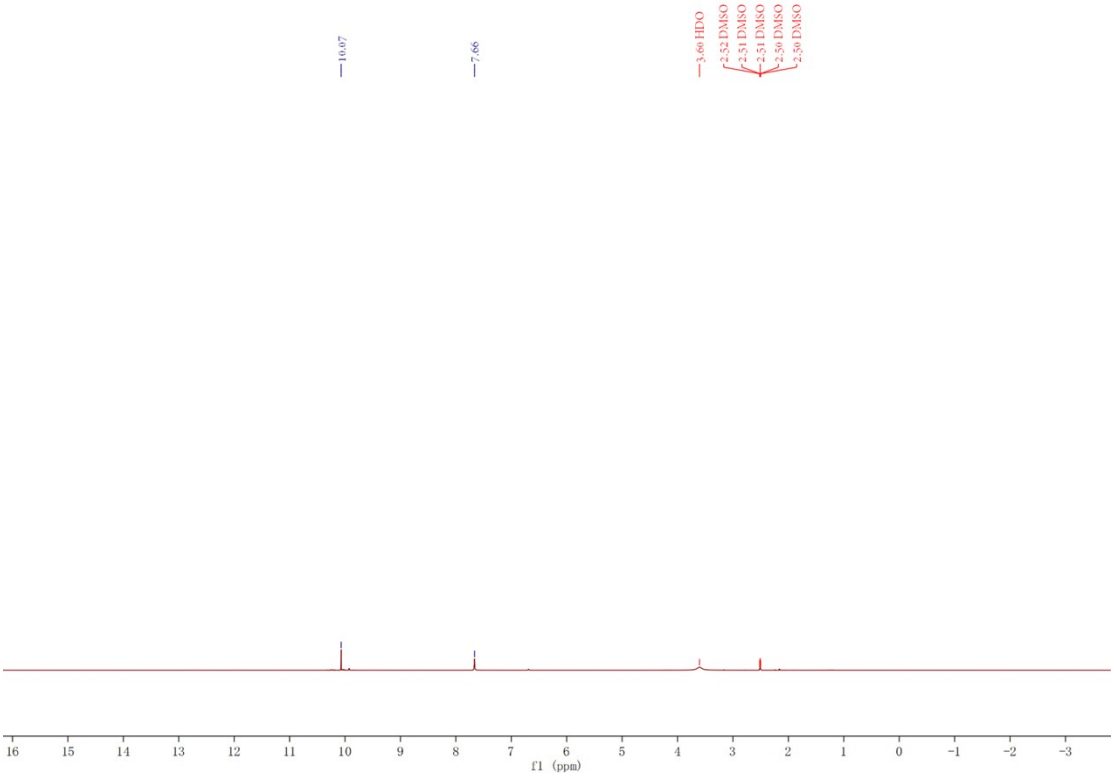

Figure S8. ^{1}H NMR spectra of **ATDT–K**.

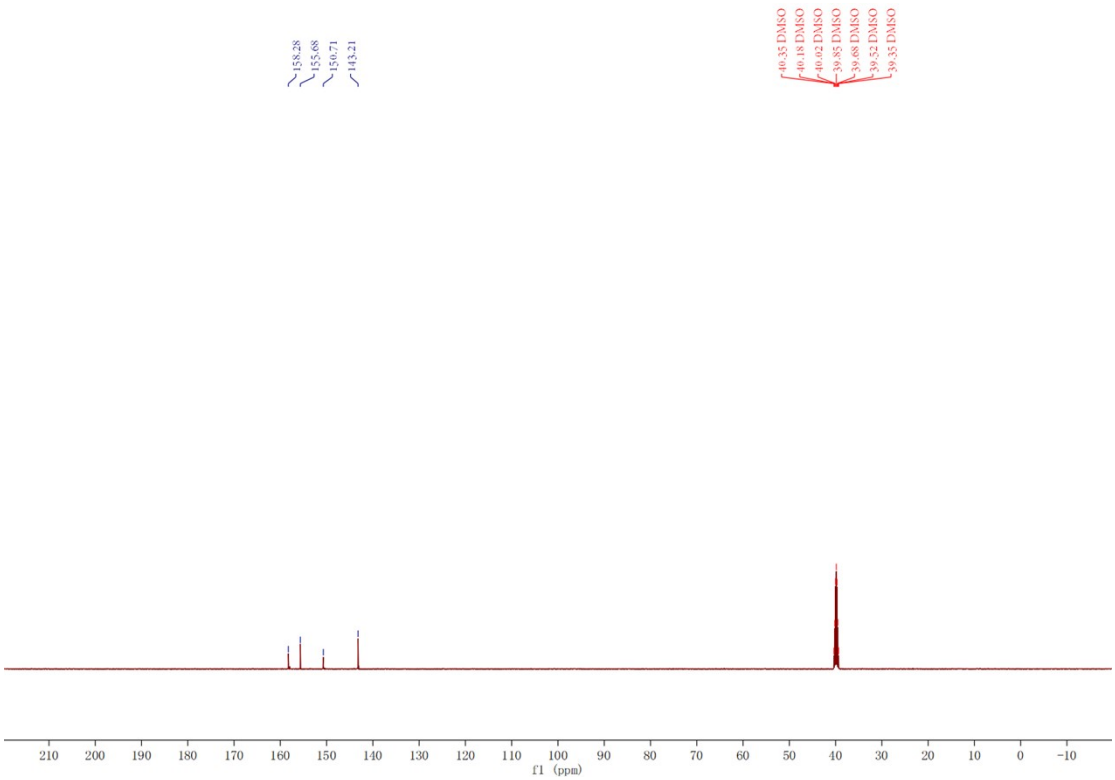

Figure S9. ^{13}C NMR spectra of **ATDT–K**.

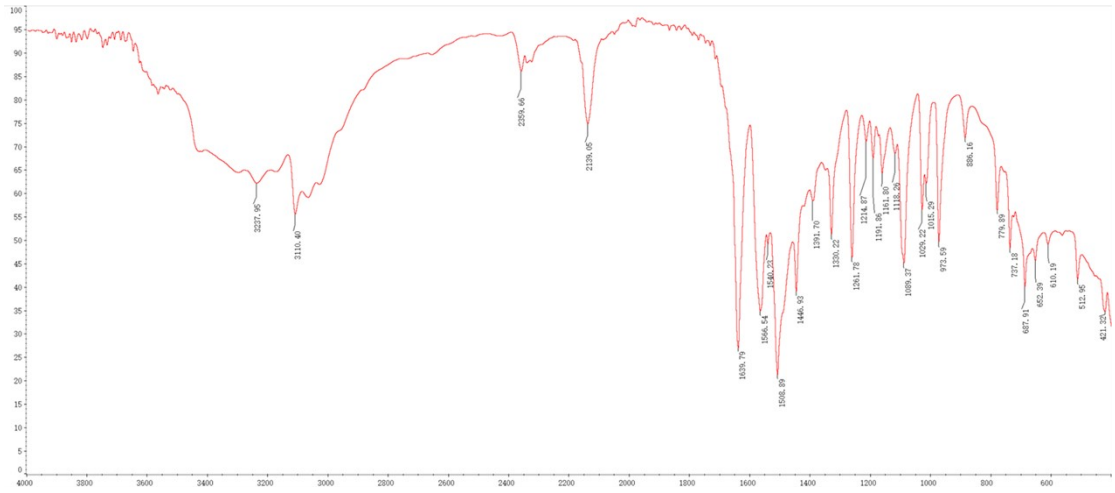

Figure S10. IR spectra of **ATDT–Rb**.

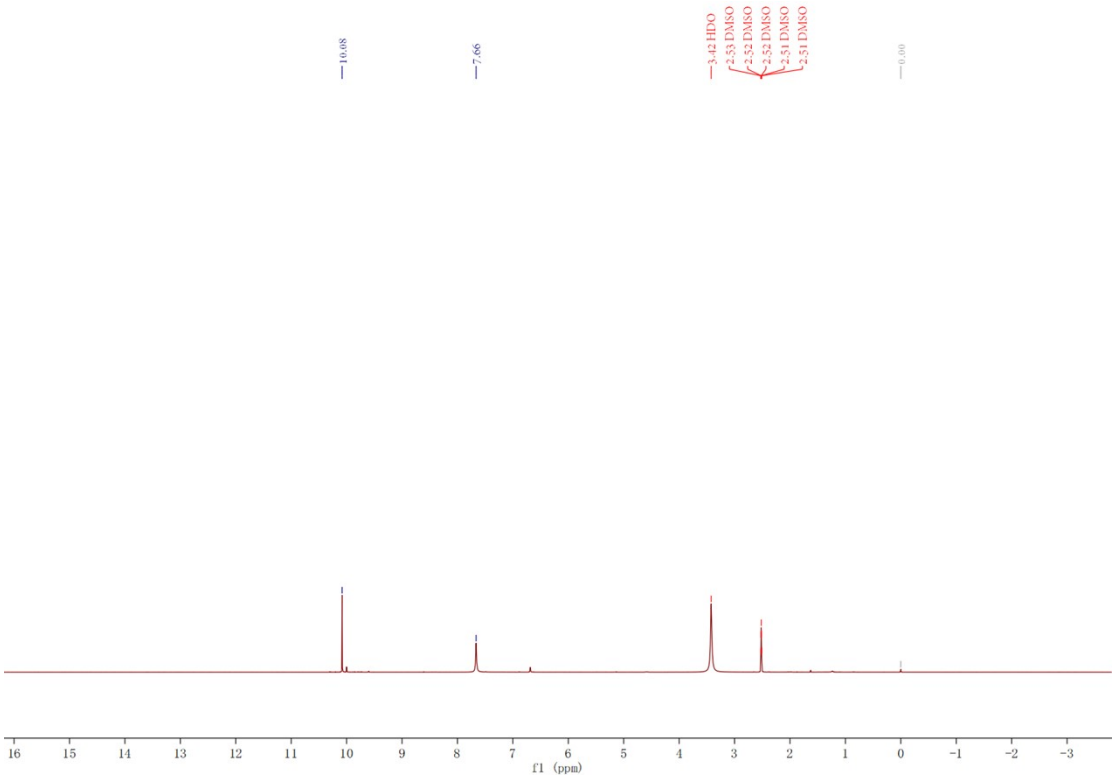

Figure S11. ^{1}H NMR spectra of **ATDT–Rb**.

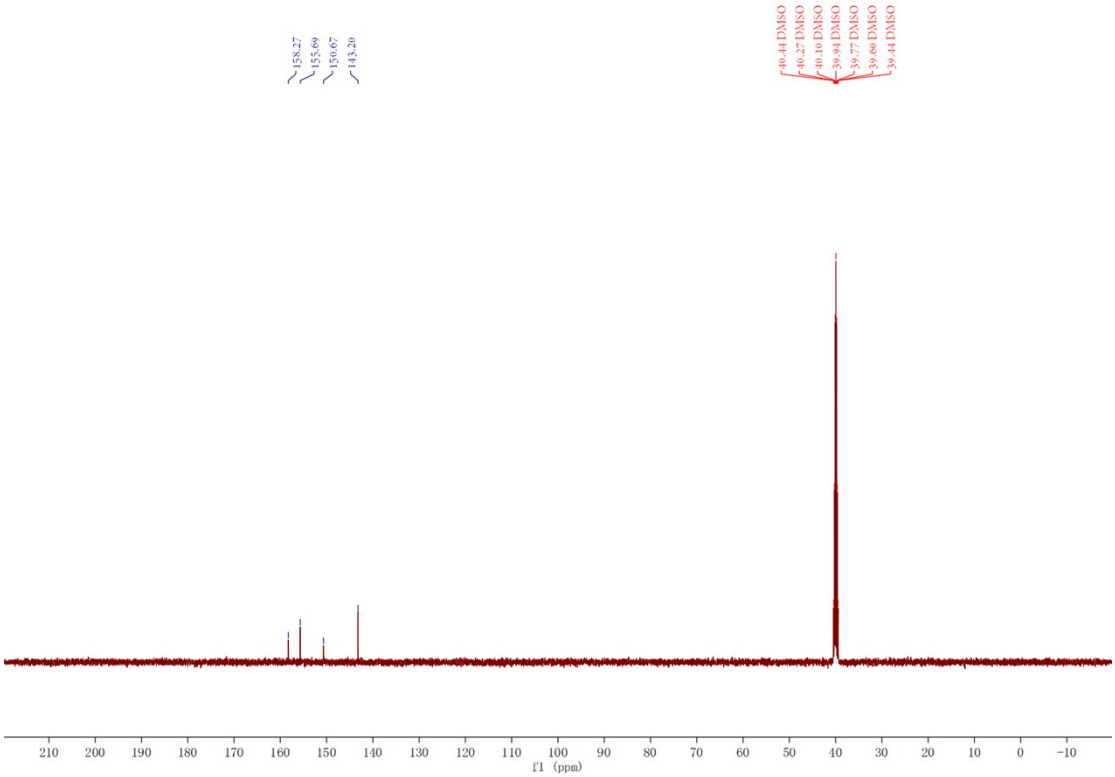

Figure S12. ^{13}C NMR spectra of **ATDT–Rb**.

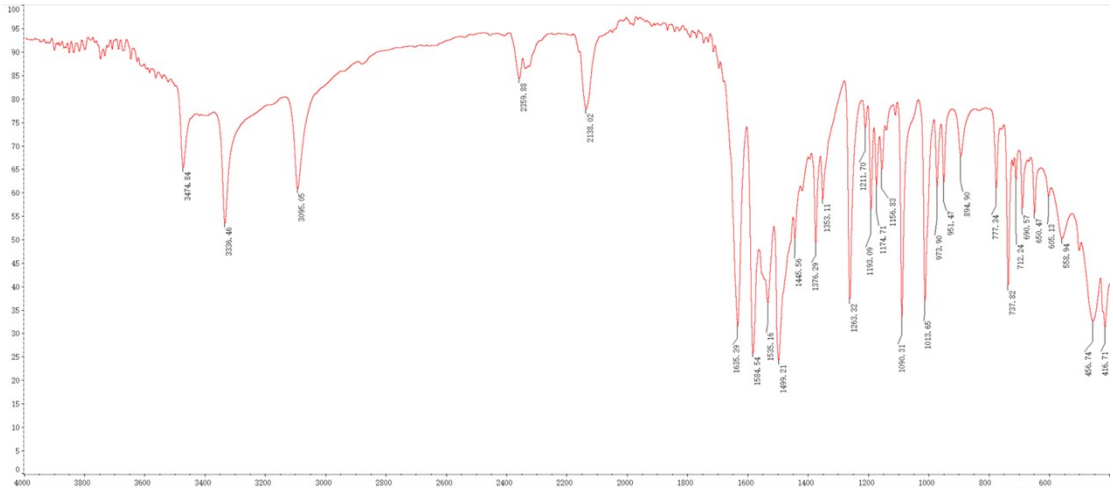

Figure S13. IR spectra of **ATDT–Cs**.

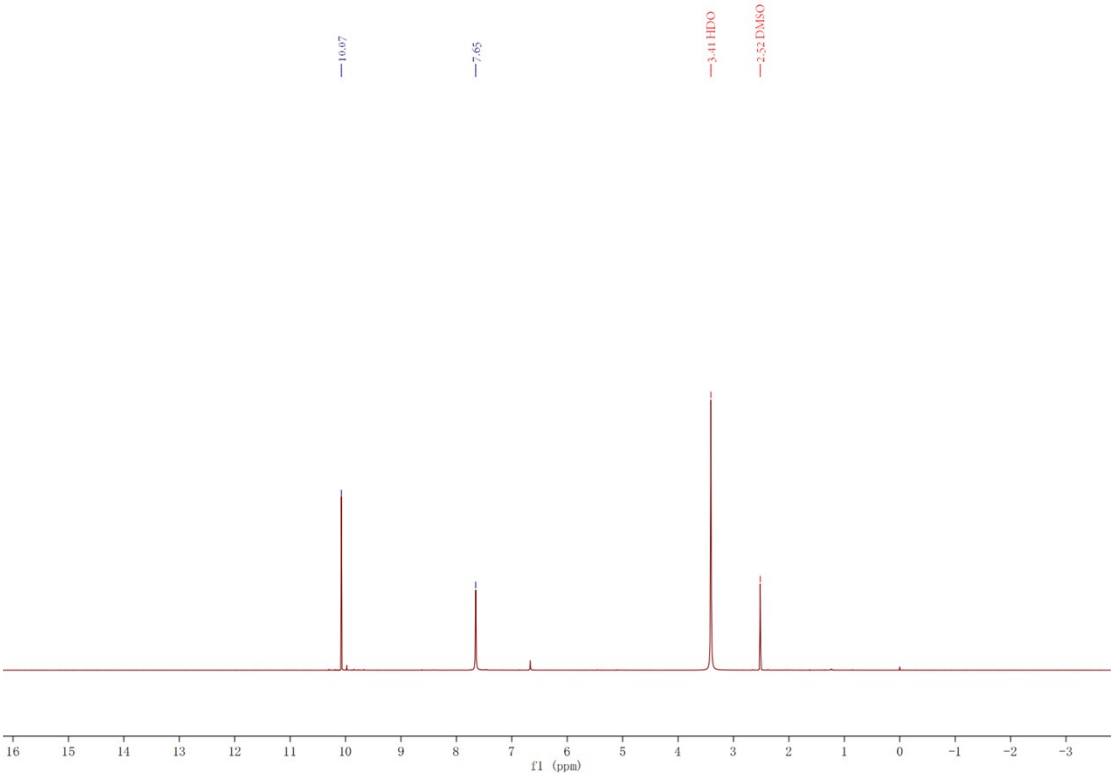

Figure S14. ^{1}H NMR spectra of **ATDT–Cs**.

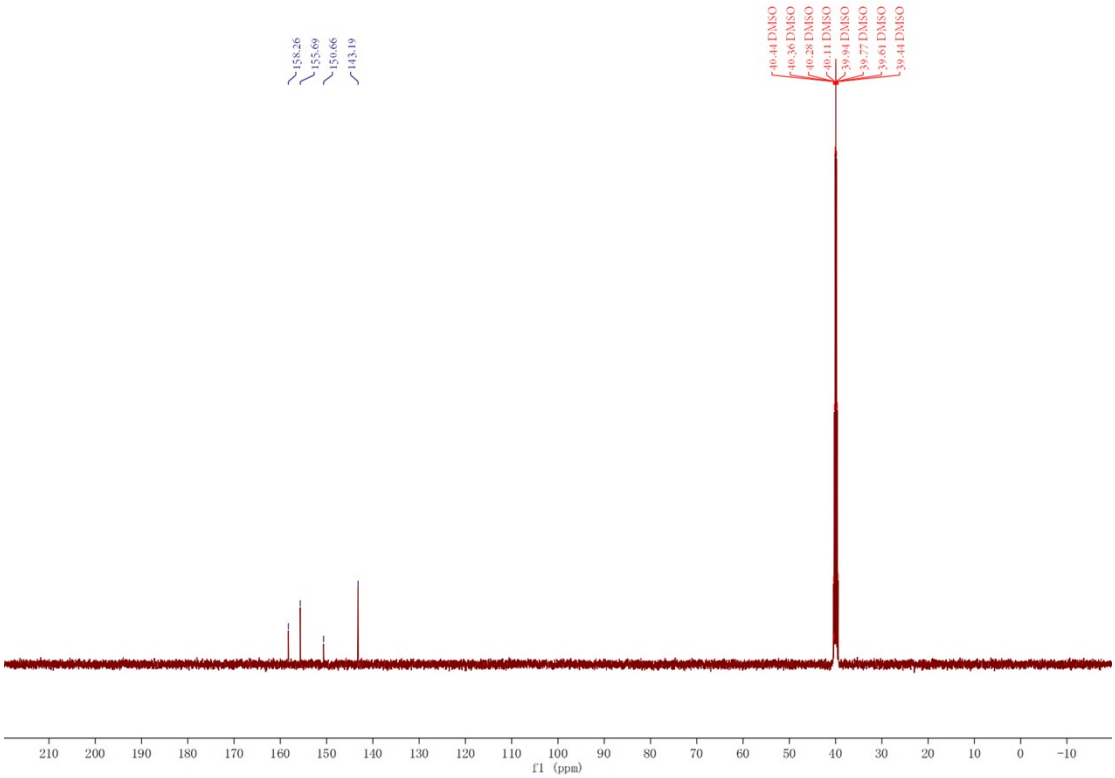

Figure S15. ^{13}C NMR spectra of **ATDT–Cs**.

3. Calculational Details

Computations were carried out by using the Gaussian 16 suite of programs.[1] The theoretical gas phase enthalpies of formation were calculated used the hybrid DFTB3LYP methods with 6-311++G** basis set based on isodemic reactions (**Scheme S1**).

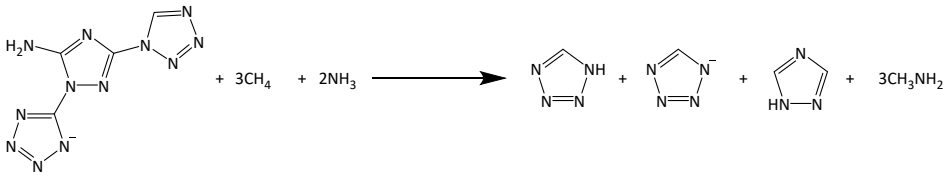

Scheme S1 Isodesmic reactions for calculating heats of formation.

For energetic salts, the solid-phase heat of formation is calculated based on a Born-Haber energy cycle (Figure S16)[2].

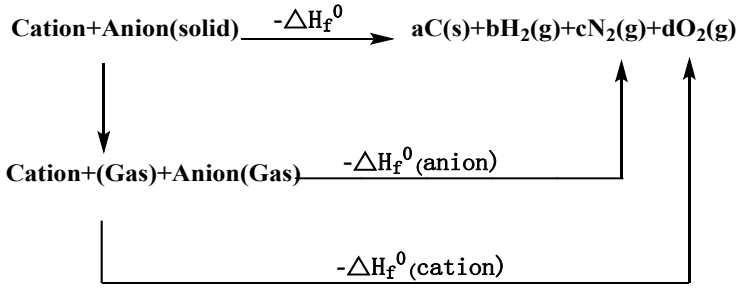

Figure S16. Born-Haber Cycle for the formation of energetic salts.

The number is simplified by equation 1:

H_f^0 (salt, 298 K) = H_f^0 (cation, 298K) + H_f^0 (anion, 298K) – H_L (1)

where H_L is the lattice energy of the salts, which could be predicted by using the formula suggested by Jenkins et al. [Eq. (2)]

$H_L = U_{POT} + [p(n_M/2 - 2) + q(n_X/2 - 2)]RT$ (2)

where n_M and n_X depend on the nature of the ions, M^{q+} and X^{p-}, and are equal to 3 for monatomic ions, 5 for linear polyatomic ions, and 6 for nonlinear polyatomic ions.

The equation for lattice potential energy U_{POT} [Eq. (3)] has the form:

U_{POT} [kJ mol^{-1}] = $\gamma(\rho_m/M_m)^{1/3} + \delta$ (3)

where ρ_m [g cm^{-3}] is the density of the salt, M_m is the chemical formula mass of the ionic material, and values for (g) and the coefficients γ (kJ mol^{-1} cm) and δ (kJ mol^{-1}) are assigned literature values.[3]

The solid-state enthalpy of formation for neutral compound can be estimated by subtracting the heat of sublimation from gas-phase heat of formation. Based on the literature,[4] the heat of sublimation can be estimated with Trouton's rule according to supplementary equation (4), where T represents either the melting point or the decomposition temperature when no melting occurs prior to decomposition:

ΔH_{sub} = 188/J mol^{-1}K^{-1} × T (4)

4. References

(1) Gaussian 16, Revision A.03, M. J. Frisch, G. W. Trucks, H. B. Schlegel, G. E. Scuseria, M. A. Robb, J. R. Cheeseman, G. Scalmani, V. Barone, G. A. Petersson, H. Nakatsuji, X. Li, M. Caricato, A. V. Marenich, J. Bloino, B. G. Janesko, R. Gomperts, B. Mennucci, H. P. Hratchian, J. V. Ortiz, A. F. Izmaylov, J. L. Sonnenberg, D. Williams-Young, F. Ding, F. Lipparini, F. Egidi, J. Goings, B. Peng, A. Petrone, T. Henderson, D. Ranasinghe, V. G. Zakrzewski, J. Gao, N. Rega, G. Zheng, W. Liang, M. Hada, M. Ehara, K. Toyota, R. Fukuda, J. Hasegawa, M. Ishida, T. Nakajima, Y. Honda, O. Kitao, H. Nakai, T. Vreven, K. Throssell, J. A. Montgomery, Jr., J. E. Peralta, F. Ogliaro, M. J. Bearpark, J. J. Heyd, E. N. Brothers, K. N. Kudin, V. N. Staroverov, T. A. Keith, R. Kobayashi, J. Normand, K. Raghavachari, A. P. Rendell, J. C. Burant, S. S. Iyengar, J. Tomasi, M. Cossi, J. M. Millam, M. Klene, C. Adamo, R. Cammi, J. W. Ochterski, R. L. Martin, K. Morokuma, O. Farkas, J. B. Foresman, and D. J. Fox, *Gaussian, Inc.*, Wallingford CT, 2016.

(2) Hariharan, P. C.; Pople, J. A. *Theor. Chim. Acta.* **1973**, 28, 213-222.